



Mallat, N.K., Zia, M.T., Mirza, N.M. and Ur Rehman, M. (2018) Ultra-wideband MIMO radio channel characterisation for body-centric wireless communication. *International Journal of Applied Engineering Research*, 13(1), pp. 40-46.

There may be differences between this version and the published version. You are advised to consult the publisher's version if you wish to cite from it.

<http://eprints.gla.ac.uk/201100/>

Deposited on: 15 November 2019

Enlighten – Research publications by members of the University of Glasgow
<http://eprints.gla.ac.uk>

Ultra-Wideband MIMO Radio Channel Characterisation for Body-Centric Wireless Communication

Nazih Khaddaj Mallat^{1, #}, Muhammad Talha Zia², Nada Masood Mirza³ and Masood Ur Rehman⁴

^{1,2,3}College of Engineering, Al Ain University of Science and Technology, United Arab Emirates (UAE).

⁴University of Bedfordshire, United Kingdom (UK).

E-mail IDs: nazih.mallat@aau.ac.ae; mohammad.zia@aau.ac.ae;
nada.mirza@aau.ac.ae; masood.urrehman@beds.ac.uk

Abstract

The channel characteristics of an on-body wireless communication system are investigated in a real-time scenario. The scattering parameters (s_{21}) are analysed of mimo antenna, for four on-body wireless channels, namely, belt-head, belt-chest, belt-wrist and belt-ankle. The body shadowing effect was added into our observation through multiple body movements at different time intervals on Ultra-Wideband (UWB) radio signals. The channel capacity of a wireless link is improved between two on-body antennas by using a 2x2 Multiple Input Multiple Output (MIMO) system in body-centric wireless communication. Further, two technique water-filling and equal powers are studied, examined and compared through simulations in terms of channel capacity for four on-body channels.

Keywords: Ultra wide band (UWB), MIMO, Wireless Body Area Networks (WBAN), On-Body Wireless Channels, IEEE 802.15.6.

INTRODUCTION

There has been a trend towards increasing application scenarios and the miniaturization of the mobile technology, personalization and the convergence of multiple functionalities into handheld communication systems as a more challenging field of scientific research [1]. Among these fast-paced trends in the communication industry, body-worn devices have emerged, opening up a new field of research called body-centric wireless communications. Communication between two or more devices on or in the human body uses the body surface as a support in the body-centric communication scenario [2].

The primary focus of this project could be formulated in the evaluation of an on-body wireless channel at the Ultra-Wideband (UWB) frequency range (3.1GHz – 10.6GHz). At this high frequency range, the observed propagation of radio waves involves two possible behaviours: first, the common behaviour of MIMO System, involves propagation through multiple paths to the receiver side across the body and also reflection through the environment and the body parts. The second propagation behaviour consists of waves creeping over surface of the body [2]. At higher frequencies propagation inside the body is negligible.

However, in the case of wireless body area network (WBANs), there is an obvious possibility that the transmitter and receiver antenna will change their positions and could contribute in degradation in received signal. In human bodies, there may be two types of movement. One is due to the movement by the body parts, for example, shaking or rubbing the hands, etc., and the other is due to the movement of the complete body movement. These two types introduce different kinds of signal degradation. Fading is due to the movement of the body parts, while scattering and polarization mismatch are due to movement by the whole body. Subjected to any transmission, the human body itself reflects the signal when it encounters certain body parts. It also causes signal strength to fade in certain areas. In the case of on-body reception, the path of the signal towards the receiver is either from the front of the body or the back, which gives rise to multipath fading. Multipath propagation in on-body propagation channels could also be observed due to the many factors in indoor environment.

The exact consideration of the specific absorption rate (SAR) is important. The requirement is to keep the transmitted power as low as possible. The acceptable SAR value is different in different parts of the world. In the US, it is 1.6 W/Kg in 1g of tissue whereas in Europe, the limit is 2.0 W/Kg in 10g of tissue [3]. In the testing scenario, the transmitted signal power is kept at 0 dBm or 1 mW, which is less than the limit in any region of the world but still quite high for the human body. There is a compulsion to keep the power level as low as possible, because this does least harm to the body and also consumes less battery power from the mounted devices.

To support high data rate transmission, multiple-input and multiple-output (MIMO) antennas are the most suitable choice. It provides increased channel capacity to deal with the application of a high data rate with less delay and better signal quality than Single input single output (SISO), Single input multiple outputs (SIMO), or multiple output single input (MISO) antennas can. It is still a little frequented area of research [4] and [5] to investigate MIMO antennas as body centric devices, and to determine the channel characterisation with respect to the Ultra-wide band frequency range. However, substantial work is being done to improve antenna design, and find how the human body could affect signal performance. Monopole antennas are examined and their behaviour is observed at the receiving end; more or less all researchers treat all the parameters as fixed rather than investigating a real life scenario [6] and [7]. The capacity comparison is achieved by

water filling, with uniform power distribution. The proposed model is based on measurements collected in the UWB frequency range using a MIMO system arrangement for different placements on the human body. The measurements are collected from four on-body channels, Belt-head, Belt-chest, belt-ankle and belt-back. For the channel matrix the observed scenarios are combined in order to replicate a user's motions, such as hand movements, breathing, talking, walking, etc., to develop a comprehensive channel model for wireless body area network.

The channel characteristics for Ultra-Wideband at the 3.1 – 10 GHz frequency range are discussed in [8], [9] and [10]. Antennas are compared with respect to path loss for the various on-body channels that are presented in [11] and [12]. For indoor use, at 846 MHz and 2.45 GHz, channel statistics are deduced for on-body and off-body channels in [13]. Channel characteristics for body-worn receivers are modelled at 5.2 GHz, according to their realization two-thirds of their observed path was Nakagami distributed, while one-third was Rician distributed. Ryckaert et al. [14] present a BAN channel model for 400 MHz, 900 MHz and 2.4 GHz with statistical simulations. Standardization bodies are still encouraging researchers to probe further into this particular area of on-body wireless channel characterisation, because there is still room for fine-tuning before any standardization begins.

DESIGN ANALYSIS FOR ULTRA-WIDEBAND TRANSMISSION

Ultra-Wideband systems are more challenging to design than narrow band systems and the development of antennas requires sophistication because of the very wide bandwidth. Typical characterization parameters for narrowband antennas are such as the radiation pattern, polarization, orientation of antennas, and return loss are directly linked to the characterization of UWB antennas. Therefore, the characterisation of UWB systems needs more specification in term of frequency range, specifically targeting the types of UWB system. The most commonly used parameter is the antenna's spatial frequency domain transfer function. Impulse response in the time domain is also a characteristic parameter for UWB antenna. The implication of a frequency transfer function to quantify the radiation pattern for a particular UWB antenna design also counts among its characteristics. The parameters specially related to the UWB antennas, plus some of the traditional design parameters including radiation, efficiency and impedance matching, are discussed below [15].

A. FREQUENCY DOMAIN TRANSFER FUNCTIONS

The mathematical expressions through which the antenna's transmit and receive transfer function can be expressed is set down as in [15], namely,

$$H_{TX}(\omega, \theta, \phi) = \frac{E_{rad}(\omega, \theta, \phi)}{V_{in}(\omega)} \quad (1)$$

$$H_{RX}(\omega, \theta, \phi) = \frac{V_{rec}(\omega)}{E_{inc}(\omega, \theta, \phi)} \quad (2)$$

$$H_{TX}(\omega, \theta, \phi) = j\omega H_{RX}(\omega, \theta, \phi) \quad (3)$$

B. SIGNAL FIDELITY

Pulse distortions introduced by the antenna, can be calculated on the basis of either frequency or time transfer function. Formulation of the fidelity between the two waveforms in the time domain, it will be defined as the normalized correlation coefficient.

$$F = \text{Max} \left[\frac{\int x(t)y(t-\tau)dt}{\sqrt{\int |x(t)|^2 dt \int |y(t)|^2 dt}} \right] \quad (4)$$

C. IMPULSE RESPONSE AND TIME SPREAD

The system design of a UWB antenna may be affected by the impulse response of each UWB antenna itself, subjected to the time domain signal shape and bandwidth. The major concern in designing a UWB antenna is what will be its effect on the human body, and vice versa. To justify the line of argument, or when investigation in a particular area requires more research, and resources are limited, the body mounted UWB antenna was first presented with decreased sensitivity [16].

MIMO ON-BODY CHANNEL MODEL

Consider a MIMO system with an M number of transmitting antennas and N number of receiving antennas.

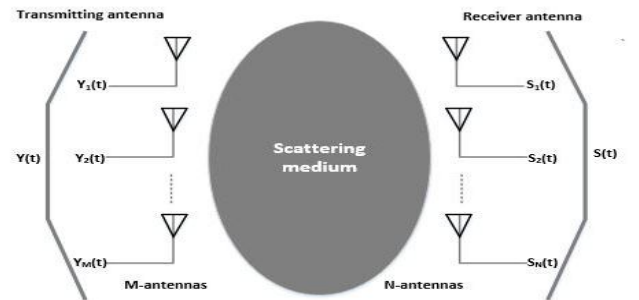


Figure 1: MIMO antenna array in scattering environment [17]

The signals generated by the transmitter unit can be denoted by the $y(t) = [y_1(t), y_2(t), y_3(t) \dots \dots, y_m(t)]$, where $y_m(t)$ denotes the signal from the m element of antenna port. The signals at the receiving antenna are $s(t) = [s_1(t), s_2(t), s_3(t) \dots \dots, s_n(t)]$, where $s_n(t)$ represent the signal at the n element of the receiving antenna port.

The radio channel in between the transmitting and receiving end denoted the relation between them.

$$H = \begin{bmatrix} \alpha_{11} & \alpha_{12} & \dots & \alpha_{1N} \\ \alpha_{21} & \alpha_{22} & \dots & \alpha_{2N} \\ \dots & \dots & \dots & \dots \\ \alpha_{M1} & \alpha_{M2} & \dots & \alpha_{MN} \end{bmatrix} \quad (5)$$

Where, α_{MN} is the complex transmission coefficient from antenna n at the receiver to the antenna m at the transmitter. For

simplicity, it is being assumed that, α_{MN} is the Gaussian distributed with equal average power [17].

Thus, the relation between the input vector $y(t)$ and the output vector $s(t)$ represented as;

$$y(t) = H(t)s(t) \quad (6)$$

A. ASSUMPTION

It is assumed throughout that the polarization and the radiation pattern of all the antennas present in the two arrays are the same. The spatial complex correlation coefficient at the transmitter between the two consecutive antenna m_1 and m_2 is denoted by:

$$\rho_{m_1 m_2}^{BS} = (\alpha_{m_1 n}, \alpha_{m_2 n}) \quad (7)$$

Where, $(\alpha_{m_1 n}, \alpha_{m_2 n})$ is the actually responsible for computing the correlation coefficient between m and n . The spatial correlation matrix at the receiving end would be achieved through the same relation.

$$\rho_{n_1 n_2}^{MS} = (\alpha_{n_1 m}, \alpha_{n_2 m}) \quad (8)$$

By the above mention coefficients the correlation matrix at the BS could be achieved as:

$$R_{BS} = \begin{bmatrix} \rho_{11}^{BS} & \rho_{12}^{BS} & \cdot & \cdot & \rho_{1N}^{BS} \\ \rho_{21}^{BS} & \rho_{22}^{BS} & \cdot & \cdot & \rho_{2N}^{BS} \\ \cdot & \cdot & \cdot & \cdot & \cdot \\ \cdot & \cdot & \cdot & \cdot & \cdot \\ \rho_{N1}^{BS} & \rho_{N2}^{BS} & \cdot & \cdot & \rho_{NN}^{BS} \end{bmatrix} \quad (9)$$

Through the correlation coefficients at the MS, the correlation matrix at the MS could be achieved as:

$$R_{MS} = \begin{bmatrix} \rho_{11}^{MS} & \rho_{12}^{MS} & \cdot & \cdot & \rho_{1N}^{MS} \\ \rho_{21}^{MS} & \rho_{22}^{MS} & \cdot & \cdot & \rho_{2N}^{MS} \\ \cdot & \cdot & \cdot & \cdot & \cdot \\ \cdot & \cdot & \cdot & \cdot & \cdot \\ \rho_{N1}^{MS} & \rho_{N2}^{MS} & \cdot & \cdot & \rho_{NN}^{MS} \end{bmatrix} \quad (10)$$

If we combine the correlation matrix, achieved through the correlation between the antennas of the transmitter and receiver the resultant correlation coefficient could be represented as:

$$\rho_{n_2 m_2}^{n_1 m_1} = (\alpha_{m_1 n_1}, \alpha_{m_2 n_2}) \quad (11)$$

This is equivalent to

$$\rho_{n_2 m_2}^{n_1 m_1} = \left(\rho_{n_1 n_2}^{MS}, \rho_{m_1 m_2}^{BS} \right) \quad (12)$$

B. THE INVESTIGATED MIMO ON-BODY SYSTEM

The 2x2 MIMO system is used to study a combine effect of possible channel characteristics under the presence of different

body parts and under different body movements. The transmitter is fixed with a belt at the waist as explained in table 1 and the receiver is kept at a different location on the body. Table 2 represents the types of body movements considered while collecting observations. A graphical representation of a 2x2 mimo system is shown in figure 2, where Tx is the transmitter side and Rx is the receiver side. However, h_{11} , h_{12} , h_{21} and h_{22} are the 2x2 mimo channel matrix parameters.

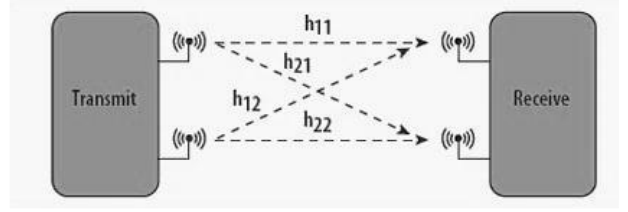


Figure 2: The 2x2 MIMO System

In our measurement setup, vector network analyser measures the scattering parameter (S_{21}) parameters of the channel between two antennas. In order to incorporate the real time multipath propagation environment, measurement is carried out in an indoor environment, where obstacles are added in order to gain multipath propagation. Planar Inverted-F antenna is used because they are more suitable in on-body communications. These antennas have an easy fabrication process, less manufacturing cost and comparatively simple structure [18]. PIFA antenna gained popularity in the application of handy wireless devices because of its compact and small size, low profile and all in-one structure [19] and when compared with other counterparts, PIFA antenna has higher inherited bandwidth.

In our measurement scenario, the signal received at the receiver end could be represented as either by the LOS or NLOS or by the combination of the both LOS and the Rayleigh distributed time varying component, depending on the on-body channel taken into observation. Therefore, the spatial sub-channel link between the j^{th} transmit element and i^{th} receive element can be formulated as [20]

$$h_{ij}(t) = \sqrt{\frac{P_r}{K+1}} \left[\sqrt{K} e^{j\phi_{ij}} + z_{ij}(t) \right] \quad (13)$$

Where, K represents the Rician factor, ϕ_{ij} represents the phase of the j^{th} and i^{th} sub-channel and $Z_{ij}(t)$ is the correlated NLOS component.

In order to acquire complete information about the channel and the formation of the link budget equation, the primary parameter of a radio wave is the path loss component. Path loss of a wireless system can be calculated by the formula

$$P_r(d) = P_r(d_o) - 10_n \log_{10} \left(\frac{d}{d_o} \right) + X_{shad}(d) \quad (14)$$

Where,

- $P_r(d_o)$ referenced distance $d_o = 1$ m subjected to average path loss

- $10n \log_{10} \left(\frac{d}{d_0} \right)$, path loss component (n) and d_0 is referenced mean path loss.
- $X_{shad}(d)$, is the zero mean Gaussian random variable representing lognormal

The (N x M) MIMO channel matrix H can be formulated through all the definition taken into consideration

$$\mathbf{H} = \begin{bmatrix} \sqrt{\frac{K_1(p_r)h}{K_1+1}} e^{j\varphi_{r1}} & \dots & \sqrt{\frac{K_1(p_r)h}{K_1+1}} e^{j\varphi_{rM}} \\ \vdots & & \vdots \\ \sqrt{\frac{K_N(p_r)h}{K_N+1}} e^{j\varphi_{N1}} & \dots & \sqrt{\frac{K_N(p_r)h}{K_N+1}} e^{j\varphi_{NM}} \end{bmatrix} + \begin{bmatrix} \sqrt{\frac{(p_r)h}{K_1+1}} z_{11}(t) & \dots & \sqrt{\frac{(p_r)h}{K_1+1}} z_{1M}(t) \\ \vdots & & \vdots \\ \sqrt{\frac{(p_r)h}{K_N+1}} z_{N1}(t) & \dots & \sqrt{\frac{(p_r)h}{K_N+1}} z_{NM}(t) \end{bmatrix} \quad (15)$$

$Z_{ij}(t)$ Is the correlated NLOS matrix component and is determined through the kronecker product of the transmitter and receiver spatial correlation matrix [20]. Since, in kronecker product the correlation coefficients are independent of the transmitter and receiver [21]. However, in an on-body wireless channel, transmitter and receiver coefficient are dependent on each other, therefore the traditional definition of the mimo channel matrix through Kronecker product is not valid. Therefore, for body area network, joint correlation matrix is being used instead of kronecker product and the result of product is as follows:

$$R = \begin{bmatrix} 1 & \alpha_{11}^{12} & \alpha_{11}^{21} & \alpha_{11}^{22} \\ \alpha_{12}^{11} & 1 & \alpha_{12}^{21} & \alpha_{12}^{22} \\ \alpha_{21}^{11} & \alpha_{21}^{12} & 1 & \alpha_{21}^{22} \\ \alpha_{22}^{11} & \alpha_{22}^{12} & \alpha_{22}^{21} & 1 \end{bmatrix} \quad (16)$$

Where, α_{ij}^{kl} is the correlation coefficient between sub-channels h_{ij} and h_{kl} . According to the pragmatic measurement α_{11}^{12} and α_{21}^{22} , whose values are for transmitting correlation, shows high measurement on-body channels because there is no local scattering, which results in de-correlation of the signals, which are transmitted. The values α_{11}^{21} and α_{12}^{22} of correlation which are received shows elevated measurement for belt chest channel and opposite for belt head channel, which proves a very weak LOS component in the latter one as compared to the former one.

The maximum throughput a MIMO systems can achieve is not same as in theory as in practice [22]. There are many limiting factors of MIMO efficiencies, such as the channel indicators, correlation, and signal to noise ratio, the antenna separation, and the relation of the number of antennas in the transmitter with those in the receiver. Let's assume that the number of antennas is fixed, and then the two important factors that can affect the outcome are the spatial correlation between the sub-channels and the average SNR received. Channel capacity is directly proportional to the SNR received. High SNR also depends upon the type of link i.e. either Line of Sight (LOS) or Non Line of Sight (NLOS). In an LOS link, high SNR is achieved, due to the small amount of signal scattering; as a result the spatial correlation between the sub-channels is reduced. A common perception about MIMO antennas is that

they are not efficient for LOS communication or rician fading because of strong correlation, but this perception is restricted to a few studies [23], where the MIMO channel capacity increases in situations of Rician fading.

RESULTS AND DISCUSSION

The 2 x 2 on-body MIMO system is analysed by the 10% outage and ergodic capacities, through waterfilling and uniformly distributed power allocation schemes. The simulation results below derive from a comparison between the measured and simulated capacities for belt-head, belt-chest, belt-wrist, and belt-ankle MIMO channels, taking the work previously done in [20], [24] and [25] as a reference. The normalization factor of all these four channels is kept same, to preserve the forbenious norm at M x N. As discussed before, all four channels act differently on one another in terms of antenna element correlation. In belt-head and belt-back on-body channels, the LOS component is comparatively less than compared to in the belt-chest on-body channel, where the correlation between the antenna elements is high.

Table 1: MIMO Antenna Position over Human Body

Transmitter Antenna Position	Reciever Antenna Position	On-Body Channel
Belt	Ankle	Belt-Ankle (BA)
	Chest	Belt-Chest (BC)
	Back	Belt-Back (BB)
	Wrist	Belt-Wrist (BW)

Table 2: Movements Done for each Channel during Measurements

Body movements	On-body channel			
	BC	BW	BA	BB
Random hand movement	✓	✓	✓	✓
Walking and Running	✓	✓	✓	✓
Eating, drinking and lifting	✓	✓	✓	✓
Siting, Standing and Exercise	✓		✓	✓
Leaning (forward, backward, sideways)	✓			✓
Typing and Writing	✓			✓
Hands on chest, side and stretching in front		✓		
Punching and Kicking			✓	
Waving, Lifting things from floor		✓		
Tighten laces and moving feet while sitting			✓	

A. BELT-ANKLE CHANNEL

Figure 3 represents the ergodic and outage capacities of belt-ankle on body channel for waterfilling and equal power allocation schemes. From this result, it may be noted that at the low SNR range belt-ankle shows similar behaviour to that of the Rayleigh fading channel. The path loss factor is high in this range because of the low LOS component present. Moreover, the waterfilling provides the optimum capacity values. The reason behind the efficiency of waterfilling is that the power is distributed optimally between the Eigen channels according to their state and to balance the disadvantage of low SNR. Whenever distribution is uniform, the power is kept at a certain value in all channels which produces an imbalance. With the waterfilling scheme, the on-body channel behaves very similarly to the Rayleigh channels when subjected to 6 dB SNR range. The capacity values achieved by both techniques are approachable at different SNR, the capacity of 2 bps/Hz is achieved at 6 dB SNR with waterfilling, but with equal power the same capacity value is achieved at 8 dB SNR. Given high SNR values, no major difference can be observed between the waterfilling and equal power distribution because the factor that determines the capacity is SNR. Therefore, from the standpoint of computational complexity, equal power would be a better choice for high SNR values because of its simplicity. However, the other factor that outweighs the complexity factor is battery consumption. It is evident that battery consumption is higher with equal power than with water filling because of the large number of iterations required to reach its mean value.

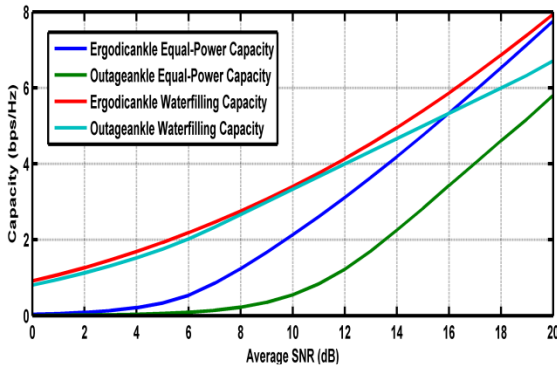


Figure 3: Comparison of different capacities of the belt-ankle on-body channel

B. BELT-CHEST CHANNEL

In Figure 4, which shows the belt-chest on body wireless channel capacities, the ergodic and outage capacities are plotted at different SNR values, using waterfilling and equal power allocation schemes. These graphs represent the same behaviour as discussed above in regard to the belt-ankle channel. These capacities and values can be understood at two levels; one represents low SNR values, where the waterfilling on equal power is dominant, affording better throughput and less computation, which causes lower consumption of battery power consumption and increases the lifetime of the battery backup. On the other hand high SNR values; still waterfilling ergodic capacity graph shows a slightly better performance than its equal power counterpart. From the graph below, it may

be concluded that the waterfilling performs better than equal power at high and low SNR. However, the difference at high SNR is not a major one. The capacity of 2 bps/Hz been achieved at 6 dB SNR values in the case of waterfilling; however, the same capacity is achieved at 11 dB SNR values in the case of equal power. Moreover, after 10 dB SNR we can see a drastically steeper curve with equal power.

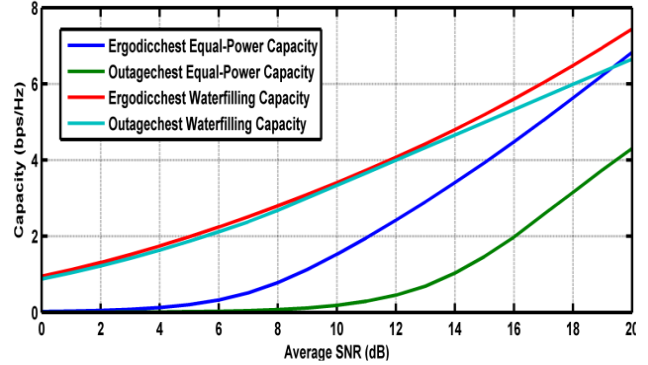


Figure 4: Comparison of different capacities of Belt-chest on-body channel

C. BELT-BACK CHANNEL

Figure 5 represents the third on-body channel, namely belt-back, where the receiver antenna is placed at the back of the human body. Here, as it is clear from the setup, the NLOS part would be present and the LOS component would be suppressed. The low spatial correlation results in the case of belt back in blurring of the antenna elements which took the channel close to the Rayleigh channel. Now, the capacity factor, as discussed in connection with the previous on-body channel, is the same. Here, waterfilling also outperformed equal power, which shows its competence in both transmission links, LOS and NLOS. Here the NLOS example is observed, while in the belt-chest case, where the LOS component is dominant, waterfilling obtains better capacity values than equal power does. In this channel, at low SNR values, the capacity values are well realized by waterfilling. However, at higher SNR, equal power approaches the waterfilling capacity values which are considered similar for further high SNR > 20 dB.

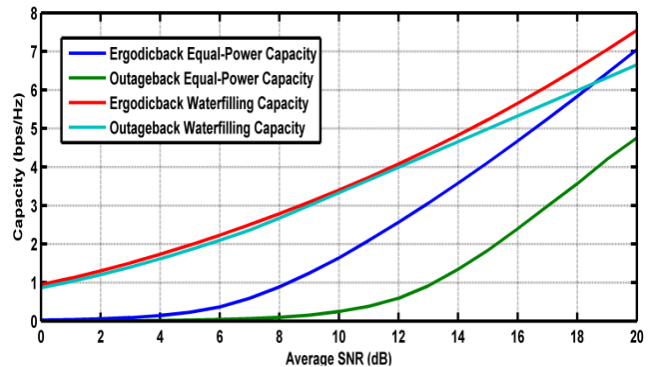


Figure 5: Comparison of different capacities of the belt-back on-body channel

D. BELT-WRIST CHANNEL

Figure 6 represents the belt-wrist channel where the receiving antenna is fixed on the wrist. This channel is important to the antenna because it is unique to its dynamic nature, because the link observed in this communication generally has some partial LOS component and some transition from the LOS to NLOS is noticed. Here, the average capacity increase is less than 1 bps/Hz per 2 dB rise in SNR. More or less the same profile of waterfilling and equal power allocation is observed, as discussed above. SNR values are the distinguishing factor for the performance of waterfilling and equal power. Equal power capacity graphs show steeping behaviour after 10 dB SNR and acquire approximately the same capacity value. For the SNR > 10 dB values, the capacity values deduced from equal power are not reliable. However, in the same scenario, waterfilling starts with reasonably good capacity values and maintains its performance up to a total of 20 dB SNR.

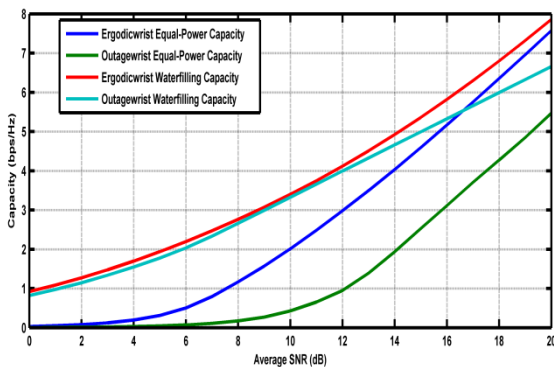


Figure 6: Comparison of different capacities of Belt-wrist on-body channel

At high SNR values, the 2x2 MIMO, the ergodic and outage capacity through waterfilling and equal power show almost the same behaviour for all the on-body channels, as previously discussed. Our main concern is the low SNR performance of the power allocation schemes; based on comparison, waterfilling produces the best capacity values and throughput. The compared capacity loss in ergodic capacity of all four channels with the Rayleigh channel [20] at fixed SNR (20 dB) is < 3 bps/Hz in the case of waterfilling and < 4 bps/Hz in the case of equal power. Capacity is directly related to the correlation between sub-channels, a sweeping effect increasing and decreasing the capacity observed in different on-body channels. Belt-chest and belt-head show high correlation among antenna elements, resulting in increased capacity values. The increment observed in average capacity is approximately 1.5 bps/Hz per 3 dB rise in SNR, compared to [25] and [27], while a 3 dB rise in SNR may be deduced due to (n x m) MIMO systems.

CONCLUSION

The advantages gained are a deeper understanding of on-body wireless channels and help in analysing the performance of the system. The channel losses due to fading and multipath propagations are then countered by the application of UWB and

MIMO antenna in our system. Four on-body channels – belt-chest, belt-wrist, belt-waist and belt-ankle – are analysed through measurements taken in real-time scenarios and simulation results. These measurements (scattering parameters) are taken at different intervals of time with multiple body movements. Body movements introduce the body shadowing effect in our measurement. The application of MIMO Planer Inverted-F Antenna (PIFA) in body-centric wireless communication is found to be very robust and effective for achieving increased capacity, as evident from the simulation results. UWB (3.1 – 10.6 GHz) radio signal use in our proposed system is also responsible for increased capacity and improved data throughput in low SNR because of the large bandwidth support. At low SNR values, the comparison is significant: waterfilling is observed to dominate with an increased throughput/data rate, producing the best capacity values.

REFERENCES

- [1] C. Baber, J. Knight, D. Haniff and L. Cooper, "Ergonomics of wearable computers," *Mobile Networks and Applications*, vol. 4, no. 1, pp. 15-21, 1999.
- [2] P. S. Hall and Y. Hao, "Antennas and propagation for body centric communications," in *Antennas and Propagation, 2006. EuCAP 2006*, Nice, France, 2006.
- [3] I. Sarvalues.com, "What is SAR and What is all The Fuss About?," [Online]. Available: <http://sarvalues.com/what-is-sar-and-what-is-all-the-fuss-about/>.
- [4] M. R. kamarudin, Y. I. Nechayev and P. S. Hall, "Performance of antennas in the on-body environment," in *Antennas and Propagation Society International Symposium, 2005 IEEE*, Washington, DC, USA, 2005.
- [5] Y. I. Nechayev and P. S. Hall, "Multipath fading of on-body propagation channels," in *Antennas and Propagation Society International Symposium, 2008. AP-S 2008. IEEE*, San Diego, CA, USA, 2008.
- [6] A. Serra, a. Guraliuc, P. Nepa, G. Manara and P. S. Hall, "Diversity gain measurements for body-centric communication systems," *International journal of MICROWAVE AND OPTICAL TECHNOLOGY*, vol. 3, no. 3, pp. 283-289, 2008.
- [7] S. L. Cotton and W. G. Scanlon, "Channel Characterization for Single- and Multiple-Antenna Wearable Systems Used for Indoor Body-to-Body Communications," *IEEE Transactions on Antennas and Propagation*, vol. 57, no. 4, pp. 980-990, 2009.
- [8] E. Pancera, "UWB antennas and channel characteristics," in *Wireless Information Technology and Systems (ICWITS), 2010 IEEE*, Honolulu, HI, USA, 2010.
- [9] N. Manositthichai and S. Promwong, "A statistical UWB transmission networks in an indoor environment for PAN systems," in *Electrical Engineering/Electronics, Computer, Telecommunications and Information Technology, 2009. ECTI-CON 2009. 6th International*

- Conference, Pattaya, Chonburi, Thailand, 2009.
- [10] P. Pagani and P. Pajusco, "Experimental Analysis of the Ultra Wideband Propagation Channel Over the 3.1 GHz - 10.6 GHz Frequency Band," in *Personal, Indoor and Mobile Radio Communications, 2006 IEEE 17th International Symposium*, Helsinki, Finland, 2006.
- [11] E. Reusens, W. Joseph and B. Letre, "Characterization of On-Body Communication Channel and Energy Efficient Topology Design for Wireless Body Area Networks," *IEEE Transactions on Information Technology in Biomedicine*, vol. 13, no. 6, pp. 933 - 945, 2009.
- [12] Y. Wang, I. B. Bonev and J. Neilson, "Characterization of the Indoor Multiantenna Body-to-Body Radio Channel," *IEEE Transactions on Antennas and Propagation*, vol. 57, no. 4, pp. 972-979, 2009.
- [13] R. Rosini and R. D'Errico, "Space-time correlation for on-to-Off Body channels at 2.45 GHz," in *Antennas and Propagation (EuCAP), 2013 7th European Conference*, Gothenburg, Sweden, 2013.
- [14] J. Ryckaert, P. De Doncker and R. Meys, "Channel model for wireless communication around human body," *Electronics Letters*, vol. 40, no. 9, pp. 543-544, 2004.
- [15] J. D. Taylor, *Introduction to Ultra-Wideband Radar Systems*, CRC Press, 1994.
- [16] A. Pellegirini, A. Brizzi, K. Ali, Y. Hao, X. Wu, C. C. Constantinou, Y. Nechayev, P. S. Hall, N. Chahat, M. Zhadobov and R. Sauleau, "Antennas and Propagation for Body-Centric Wireless Communications at Millimeter-Wave Frequencies: A Review [Wireless Corner]," *IEEE Antennas and Propagation Magazine*, vol. 55, no. 4, pp. 262-287, 2013.
- [17] L. S. Jean Philippe Kermoal, "A Stochastic MIMO Radio Channel Model With Experimental Validation," *SELECTED AREAS IN COMMUNICATIONS*, vol. 20, no. 6, 2002.
- [18] J. H. Y. Byung Chan Kim and H. D. Choi, "Small wideband PIFA for mobile phones at 1800 MHz," *Vehicular Technology Conference, 2004. VTC 2004-Spring. 2004 IEEE 59th*, vol. 1, pp. 27 - 29, 2004.
- [19] F. D. Z. Wang, Q. Wang and K. Gong, "Enhanced-bandwidth PIFA with T-shaped ground plane," *Electronics Letters*, vol. 40, no. 23, pp. 1504 - 1505 , 2004.
- [20] K. I. Ghanem, P. Hall and L. Hanzo, "MIMO Stochastic Model and Capacity Evaluation of On-Body Channels," *Antennas and Propagation, IEEE Transactions*, vol. 60, no. 6, pp. 2980 - 2986, 2012.
- [21] B. L. L. Maharaj and J. Wallace, "MIMO Channel Modelling: The Kronecker Model and Maximum Entropy," *Wireless Communications and Networking*, pp. 1525-3511 , 2007.
- [22] Gans, G. J. Foschini and M. J., "On Limits of Wireless Communications in a Fading Environment when Using Multiple Antennas," *Wireless Personal Communications*, vol. 6, pp. 311-335, 1998.
- [23] D. Neiryneck, C. Williams and M. Beach, "Experimental capacity analysis for virtual antenna arrays in personal and body area networks," 2005.
- [24] K. Ghanem and P. S. Hall, "Investigation of capacity of on-body channels using MIMO antennas," in *Antennas & Propagation Conference, 2009. LAPC*, Loughborough, UK, 2009.
- [25] K. Ghanem and P. Hall, "Capacity Evaluation of On-body Channels Using MIMO Antennas," in *Wireless and Mobile Computing, Networking and Communications, 2009. WIMOB 2009. IEEE International Conference*, Marrakech, Morocco, Morocco, 2009.
- [26] I. Khan, "Diversity and MIMO for body-centric wireless communication channels," Ph.D. thesis, University of Birmingham, Birmingham, 2009.
- [27] I. Khan, P. S. Hall, Y. I. Nechayev and L. Akhoondzadeh-Asl, "Multiple antenna systems for increasing on-body channel capacity and reducing BAN-to-BAN interference," in *Antenna Technology (iWAT), 2010 International Workshop*, Lisbon, Portugal , 2010.